Revista Mexicana de Astronomía y Astrofísica, **00**, ??–?? ()

IMAGING AND SPECTROSCOPY OF ARP 104: A POST-STARBURST INTERACTING PAIR WITH CROSS-FUELLING?

Nathan Roche,[1]

Received 5th February 2008; accepted 5th February 2008

RESUMEN

Nathan Roche: Observatorio Astronomico Nacional, Instituto de Astronomía, Universidad Nacional Autónoma de México, Ensenada, Apartado Postal 3–72, 22860 Ensenada, Baja California, México (ndr@astrosen.unam.mx)

now at: Astronomy and Cosmology Research Unit, School of mathematical Sciences, University of KwaZulu-Natal, Durban 4041, South Africa (roche@ukzn.ac.za).

ABSTRACT

We perform UBR imaging and optical spectroscopy of the interacting galaxy pair Arp 104, at $z = 0.0098$. This consists of NGC5218, a disturbed spiral with $r_{exp} \simeq 2.53$ kpc, a substantial bulge component and an inclined outer 'shell', the round spheroidal NGC5216, a connecting bridge of length ~ 50 kpc and a curved plume. Neither galaxy shows emission lines. NGC5218 has strong Balmer lines and appears to have undergone a major starburst (3.2×10^9 $M_\odot$) some ~ 0.2 Gyr ago, triggered by the last close passage of the two galaxies. The galaxy is very red in its centre, suggesting it is dusty, but its outer regions, and the bridge connecting the two galaxies, have the blue colours of 0.2–0.4 Gyr old stars. NGC5216 lacks strong Balmer lines but outside its centre is blue in $U - B$, suggesting it experienced a star-formation episode only ~ 40 Myr ago. This could have been fuelled by gas from NGC5218, transfered through the bridge. The bridge passes through NGC5216 to emerge as a plume extending ~ 14 kpc to the SW of NGC5216. The plume, from its colours, is very young and may be a site of ongoing star-formation or the formation of a tidal dwarf galaxy.

Key Words: **GALAXIES: INTERACTING**

1. INTRODUCTION

Mergers and interactions are a very major influence on galaxy evolution, triggering bursts of star-formation and nuclear activity, and causing permanent morphological transformation. The evolution induced by galaxy interactions can reveal much about the structure of galaxies and the factors influencing their star-formation rate (SFR). For example, the long-tailed pair of spirals known as 'The Mice' (NGC4676) contains a large number of star clusters formed $1.5–2.0 \times 10^8$ yr ago (de Grijs et al. 2003), an age corresponding to the point when, according to models of the system's kinematics, the two galaxies last underwent closest passage. The starburst in the Mice appears to have been sharply peaked in time but spatially distributed throughout the system, and Barnes (2004) concluded that it was better represented by a model where the star-formation in the burst is 'shock induced' (dependent on the rate of energy input from shocks), than by a model where the SFR is solely a function of local gas density (i.e. the simple Schmidt law).

In this paper we present observations of the relatively little-studied interacting galaxy pair Arp 104, consisting of a spiral (NGC5218: type SBb-pec) and a spheroidal (NGC5216: type E0). The system was first described by Keenan (1935) who noted that the galaxies were connected by 'a faint but definite band of nebulosity', which continues beyond NGC5216 as a 'short curved arm' extending SW. It was included in the catalog of Arp (1996) in the category of 'E and e-like galaxies connected to spirals'.

[1]OAN, Instituto de Astronomía, UNAM, Ensenada, México.

NGC5218 is at RA $13^h32^m10^s.4$, Dec +62 : 46 : 04 and NGC5216 lies 4.05 arcmin away at RA $13^h32^m06^s.9$, Dec +62:42:02. The respective redshifts (recession velocities) from the Sloan Digital Sky Survey (2003) are $z = 0.009783$ (2933 ± 22 km s^{-1}) and $z = 0.009804$ (2939 ± 26 km s^{-1}); these are almost identical, meaning the relative motion of the two galaxies is approximately transverse to the line of sight with very little radial component. For $H_0 = 70$ km s^{-1} the proper distance is 41.9 Mpc, the distance modulus 33.13 mag, and 1 arcsec will subtend 201 pc.

NGC5218 was detected by IRAS with $F_{60\mu\mathrm{m}} = 6.908 \pm 0.276$ Jy and $F_{100\mu\mathrm{m}} = 14.11 \pm 0.56$ Jy (Moshir et al. 1990). From the relation of Helou et al. (1985), the IRAS fluxes correspond to a total far-infra-red flux $F_{FIR} \simeq 1.26 \times 10^{-11}(2.58 f_{60} + f_{100}) = 4.02 \times 10^{-10}$ ergs cm^{-2}s^{-1} and from this the luminosity $L_{FIR} = 8.59 \times 10^{43}$ ergs s^{-1}. From the relation of Kennicutt (1998) this corrresponds to a SFR of 3.9 M$_\odot$yr^{-1}. NGC5216 was not detected in the FIR.

Arp 104 was imaged in HI with the VLA as part of the 'rogues gallery' of Hibbard et al. (2001). The 21cm map of the system shows the HI distribution to be strongly peaked within the disk of NGC5218, with substantial amounts of gas also associated with the faint northern plume of this galaxy and the bridge between the two galaxies. The HI density falls to a minimum at the position of NGC5216, but on the other side of this galaxy there is an increase in HI density associated with the curved plume extending to the SW.

Cullen, Alexander and Clemens (2003) observed Arp 104 in neutral hydrogen and estimated that NGC5218 contains 7.8×10^9M$_\odot$ of HI. The HI kinematics show the sense of rotation as receding on the east side, with a rotation curve flattening in the outer galaxy at a maximum line-of-sight velocity component of 140–150 km s^{-1}.

Olsson, Aalto and Hüttemeister (2005) observed the centre of NGC 5218 in CO 1-0. They found a rotating ring of molecular gas, 3.5 kpc across, with a position angle 78 deg and estimated its mass as 2.4×10^9M$_\odot$. They concluded that the prominent bar of this spiral, which has a similar position angle, acts to transport gas inwards to this ring. From the high HCN/HCO$^+$ emission-line ratio at the very centre they infer the possible presence of an AGN.

Cullen, Alexander and Clemens (2006) observed Arp 104 in CO 1-0 and estimated that NGC5218 contains a total of 6.9×10^9M$_\odot$ of H_2, whereas for NGC5216 they do not detect molecular gas and set an upper limit $M_{H_2} < 7.6 \times 10^7M_\odot$. They also estimate the time since the pair experienced a close passage (perigalacticon) as 3×10^8 yr.

In this paper we aim to obtain a clearer picture of the nature and history of this interacting system through direct imaging in UBR passbands and spectroscopy of both galaxies. In Section 2 we describe our observations and data reduction. Sections 3, 4 and 5 will deal with the structure, spectra and colours of the galaxies. In Section 6 we summarise, and discuss the possible evolution of the system. Throughout $H_0 = 70$ km $s^{-1}Mpc^{-1}$.

2. OBSERVATIONS

2.1. *Data*

All observations were performed using the 0.84m telescope at the Observatorio Astronomico Nacional, situated at 2790m in the Sierra San Pedro Martir, Baja California, Mexico. The direct imaging observations were obtained on the nights of 1 and 2 May 2005 using a Marconi CCD, binned 2×2 to give an image area of 1024^2 pixels of size 0.475 arcsec. The 8.1 arcmin FOV is just sufficient to accomodate both galaxies and the associated tidal features within a single pointing.

We observed with 3 of the the standard Johnson filters installed in the 'Mexman' filter wheel of this telescope, $U3$ ($\lambda_{mean} = 3640$Å), $B3$ (4330Å) and $R3$ (6470Å). Our total usable data consisted of 10×600s exposures in B, 4×600s in R, and one 900s plus 4×1200s in U. For flux calibration, the Landolt (1992) standard star 104-461 was observed. We calibrate in Vega-system magnitudes and use these throughout this paper. Using the filter response curves we calculate the conversions into the AB system as $(U, B, R)_{AB} = (U, B, R)_{Vega} + (0.765, -0.062, 0.181)$.

The spectroscopic observations were carried out on the night of 20 May 2005 using a small Bollers and Chivens spectrograph (known as 'Bolitas'), fitted with a SITe1 CCD (1024^2 pixels, used unbinned) and an RGL grating set at an angle of approximately 6 degrees to cover the spectral range 3500Å to 5860Å. A slit of width 160μm was used, aligned E-W. To obtain a relative flux calibration we obtained (through the same slit) spectra of the spectrophotometric standard star Theta Virginis. For wavelength calibration, spectra were taken of a HeAr arc lamp. In total, we obtained 6×1200s exposures with the slit on NGC5218 and 4×1200s exposures on NGC5216.

2.2. *Data Reduction: Imaging*

Data reduction was carried out using IRAF. The direct imaging data were debiased, and then flat-

fielded using twilight sky flats. The 4 R-band and 4 U-band exposures, all taken on the clear night of 2 May, were spatially registered and combined with 'sigclip' cosmic-ray rejection. Of our 10 B-band exposures, 3 had been obtained on 2 May but the other 7 on the night of 1 May, when thin cloud was present, resulting in somewhat non-photometric conditions. We attempt to correct our photometry for this by comparing the fluxes of bright (non-saturated) stars in each of these seven images with their mean fluxes on the 3 B-band exposures from 2 May. Following this, the B-band exposures from 1 May were scaled up, and weighted down, by compensatory factors of between 1.059 and 1.225, and then combined with the 2 May data. This produces a combined B-band image with a normalization closely approximating that of the 2 May data, or that which would have been obtained in photometric conditions.

The resolution of our combined images is approximately 1.65 arcsec FWHM for B and 1.9 arcsec in R and U.

From imaging of the standard star 104-461 on 2 May we derived photometric zero-points, and applied to these a correction for Galactic extinction at this position in the sky; 0.113 mag in U, 0.089 mag in B and 0.055 mag in R, according to Caltech NED. This gave corrected zero-points, for 1 count sec^{-1}, of 20.638 in U, 22.438 in B and 22.235 in R.

2.3. *Data Reduction: Spectra*

The spectroscopic data were debiased and flat-fielded. Twilight sky flats were taken through the same slit/grating configuration as used for the observations. In the flat-fielding of spectroscopic data the aim is to remove the pixel-to-pixel sensitivity variations but not the variation along the wavelength direction. To do this, each pixel of the sky-flat was divided by the average value in its column (i.e. of all pixels at the same wavelength, averaged along the slit length), to produce a normalized flat-field with all wavelength dependence removed.

Spectroscopic observations of the standard star Theta Virginis were spatially registered and combined, the 1D spectrum extracted (using IRAF 'apall'), wavelength-calibrated (using the associated HeAr arc), and, together with the tabulated spectral energy distribution for this star (Hamuy et al. 1994), used to derive a sensitivity (relative flux calibration) function.

The 6 1200s exposures of NGC5218 and 4 of NGC5216 were spatially registered and combined with 'sigclip' cosmic-ray rejection. The 1D spectra of the two galaxies were extracted using 'apall' (with summation across large apertures spanning the visible widths of the galaxies), wavelength calibrated (using HeAr arcs) and flux calibrated in relative F_λ (using Theta Virginis). For each spectrum, we estimated an error function by extracting spectra from the individual exposures, finding the scatter between these at each pixel, dividing by $(N_{exp})^{\frac{1}{2}}$ and (as this was noisy) smoothing in wavelength.

3. STRUCTURE OF NGC5216 AND NGC5218

Figure 1 shows our combined 6000s B-band image of the Arp 104 system. Structurally, NGC5216 appears to be a simple round spheroidal, whereas the spiral NGC5218 is much more complex with a nucleus, disk, bar, and an outer 'shell'. The disk appears to lack distinct spiral arms but instead shows a ring of diameter $\sim$ 68 arcsec, about the length of the bar. The shell is an ususual feature for a spiral and is greatly (35–40 degrees) inclined with respect to the disk plane, implying it originated in a major perturbation, presumably an earlier close encounter with NGC5216. A further conspicuous interaction feature is the bridge connecting the two galaxies, which appears to pass through NGC5216 and extend SW to form a bright plume, curving increasingly towards its tip some 70 arcsec from the spheroid's centre. In the other direction, the bridge continues beyond NGC5218 northward as a fainter, more diffuse plume.

3.1. *Isophotes*

As a first characterization of the structure of the galaxies, we fitted the B-band images with concentric elliptical isophotes, using IRAF 'isophot.ellipse'. Figure 2 shows for NGC5218 the isophote surface brightness (SB), ellipticity and position angle (PA) as a function of semi-major axis (r_{sm}), together with the best-fitting exponential profile, which has a scale-length 14.68 arcsec (2.95 kpc) and central SB 20.19 B mag arcsec^{-2}.

However, the profile of NGC5218 does not closely follow a single exponential. At $r_{sm} < 16$ arcsec, the bar, with PA $\simeq 115°$, is dominant, giving isophotes with a high ellipticity (0.8) and a SB almost flat with radius. At larger radii the isophotes trace an exponential-profile disk with ellipticity $\sim$ 0.47 (corresponding to a disk inclination $\sim$ 30°), and PA $\simeq 67°$. At the largest radii, $45 < r_{sm} < 75$ arcsec, the isophotes trace the outer shell, which is rounder with ellipticity $\sim$ 0.3 and a PA $\sim 105°$, twisted $\sim$ 38 deg relative to the disk plane.

As NGC5216 is a spheroidal rather than a disk, we fit the isophotal profile with a de Vaucouleurs (or

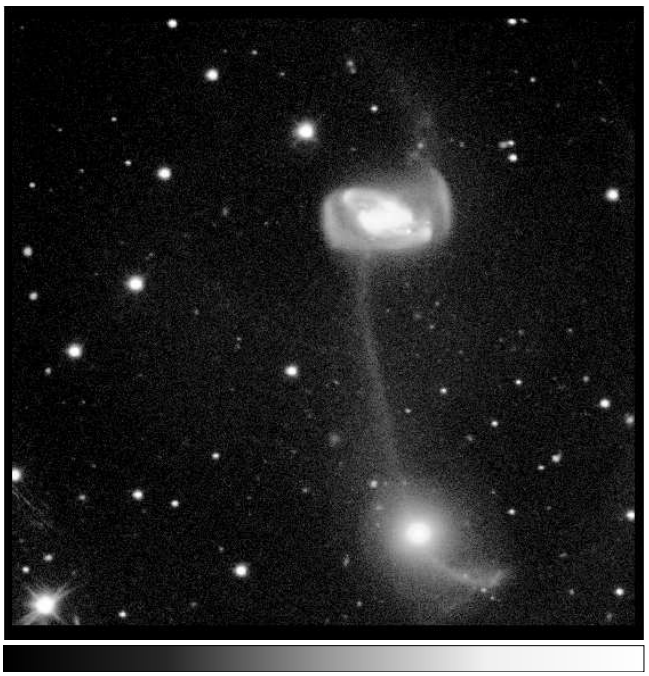

Fig. 1. B-band image of Arp 104 with total 6000s exposure time. The intensity scale is logarithmic. The image shows a 7.89×7.73 arcmin area with NGC5218 (upper) and NGC5216 (lower). N is top, E is left.

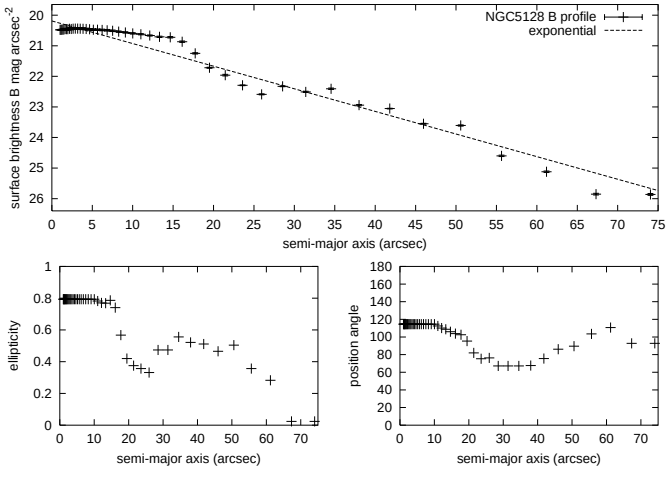

Fig. 2. Parameters of elliptical isophotes fit to NGC5218 in the B-band: surface brightness against semi-major axis (points) and best-fitting exponential (straight line); ellipticity, and position angle (in degrees anticlockwise from the North).

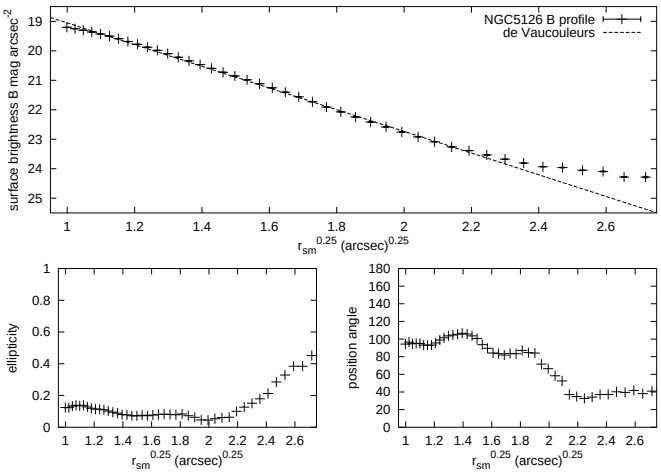

Fig. 3. Parameters of elliptical isophotes fit to NGC5216 in the B-band: surface brightness against $r_{sm}^{0.25}$ in arcsec$^{0.25}$ (points), best-fitting de Vaucouleurs profile (straight line); ellipticity, and position angle (degrees anticlockwise from the North).

Sersic $n = 4$) profile. Figure 3 shows the isophote SB, ellipticity and PA against $r_{sm}^{0.25}$. This galaxy is almost round (ellipticity ~ 0.1), and the SB is close to the $r_{sm}^{0.25}$ law (i.e. a straight line on this graph) out to $r \simeq 20$–25 arcsec. At larger radii the SB shows an excess above the $r_{sm}^{0.25}$ law, the ellipticity rises sharply and the PA moves to $\sim 35°$, all due to the influence of the bridge/plume on the isophotes at large radii. To minimise this, we fit our model profile to only the $0 < r_{sm} < 20$ arcsec isophotes.

The de Vaucouleurs profile is customarily parameterized in terms of an 'effective intensity' I_{eff}, 8.325 magnitudes fainter than the SB at $r = 0$, and the radius r_{eff} at which the isophote SB is I_{eff}. For our profile best-fit to NGC5216, $I_{eff} = 23.70$ B mag arcsec^{-2} and $r_{eff} = 26.2$ arcsec or 5.27 kpc. For NGC5218, integrating the flux out to the $r_{sm} = 74$ arcsec isophote gives the total magnitude as $B = 12.946$ with integrated colours $U - B = 0.24$ and $B - R = 1.25$, and a half-light radius of 22.9 arcsec (4.60 kpc). For NGC5216, integrating out to $r_{sm} = 41$ arcsec gives $B = 13.884$ with integrated colours $U - B = 0.23$ (similar) and $B - R = 1.44$ (redder), and $r_{hl} = 12.0$ arcsec (2.4 kpc). At the distance of this system these B magnitudes correspond to absolute magnitudes $M_B = -20.20$ for NGC5218 and $M_B = -19.30$ for NGC5216, taking into account k-corrections of 0.020 mag and 0.054 mag respectively, as calculated directly from our observed spectra (Section 4).

	NGC5218		NGC5216
	disk	bulge	bulge
Sersic n	1.0	1.729	3.679
r_{exp}	12.61	-	-
r_{eff}	-	46.81	27.34
μ_{cent}	20.28	-	-
μ_{eff}	-	25.28	23.81
Ellipticity	0.491	0.155	0.009
Posn. Angle.	68.8	68.7	86.9
Lum. fraction	0.695	0.305	1.0

3.2. *Bulge/Disk Decomposition*

We can perform a more sophisticated fitting using BUDDA (Bulge/Disk Decomposition Analysis), a program developed by de Souza, Gadotti and dos Anjos (2004). This program fits galaxies in 2D, rather than as a 1D radial profile, iteratively converging on the best-fitting combination of an exponential disk and a bulge of generalized Sersic index. BUDDA assigns to each component a separate flux, position angle and ellipticity. It also generates an image of the model which can be subtracted from the real galaxy to highlight the residuals (e.g. bars, spiral arms, or point sources). Using BUDDA we fit the B-band image of NGC5218 with a disk plus bulge combination. NGC5216 was found to lack any significant disk component and so we fitted with a single-component bulge. Table 1 gives the parameters of the BUDDA best-fits.

NGC5218 is a spiral with a substantial bulge component; the B-band luminosity ratio is $B/D = 0.429$, within and toward the upper end of the range for its Hubble type $T = 3$/Sb (e.g Giuricin et al. 1995). The bulge component of NGC5218 has the same PA as the disk and is a 'normal' part of the galaxy, in contrast to the outer shell (Figure 4) for which the PA ($\sim 105°$) is twisted 38° anticlockwise with respect to the disk, indicating it is produced tidally by the interaction. For the disk component $r_{exp} = 2.53$ kpc.

The BUDDA best-fit parameters for NGC5216 are very close to those obtained by fitting the isophotes with a fixed $n = 4$, and confirm the E0 classification (i.e. $n \sim 4$; ellipticity~ 0). The residuals with respect to the BUDDA model fit are a reduced χ^2 of only 2.17 for NGC5216 but 23.51 for NGC5218, reflecting its later type and complex and disturbed morphology.

Figures 4 and 5 show the two galaxies' residuals, i.e the observed B-band images with the best fit BUDDA models subtracted. In NGC5218 the brightest residual features (~ 21 B mag arcsec^{-2}) are at the two ends of the bar, followed by the outer ring of the disk, and the 'shell' (~ 23 B mag arcsec^{-2}) where seen well out of the disk plane. It is also notable that the connecting bridge curves to apparently pass through the nucleus perpendicular to the disk and emerge as the more diffuse northern plume.

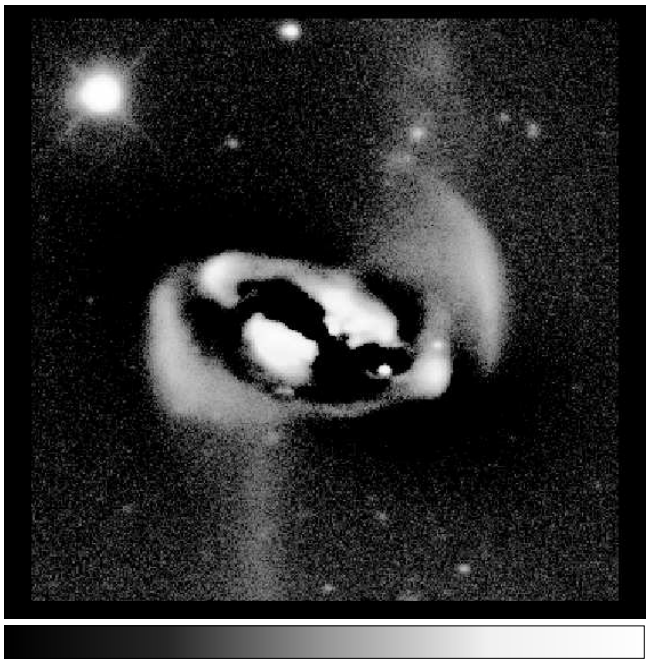

Fig. 4. B-band image of NGC5218 with the BUDDA best-fit disk plus bulge model subtracted. The area shown is 161 × 161 arcsec, with a log intensity scale.

In NGC5216 the only residual associated with the galaxy itself is a central bright spot. However, the bridge is clearly seen to pass through the nucleus of the galaxy and emerge to the SW as a curved plume of high SB (reaching 23.7 B mag arcsec^{-2}), which abruptly bends and terminates 70 arcsec (14kpc) from the nucleus.

4. SPECTROSCOPY; AGE-DATING THE STARBURST

Figures 6 and 7 show our 'Bolitas' spectra of NGC5218 and NGC5216, with detectable features labelled. The continuum signal/noise at $\lambda > 4200$Å is $\sim 18\sigma$ for NGC5218 and $\sim 9\sigma$ for NGC5216. These spectra are plotted with only a relative flux calibration as the slit will capture only a fraction of the flux from each galaxy. However, if we assume that the region of each galaxy covered by the slit is representative of the whole object, we can estimate an approximate whole-galaxy absolute calibration by

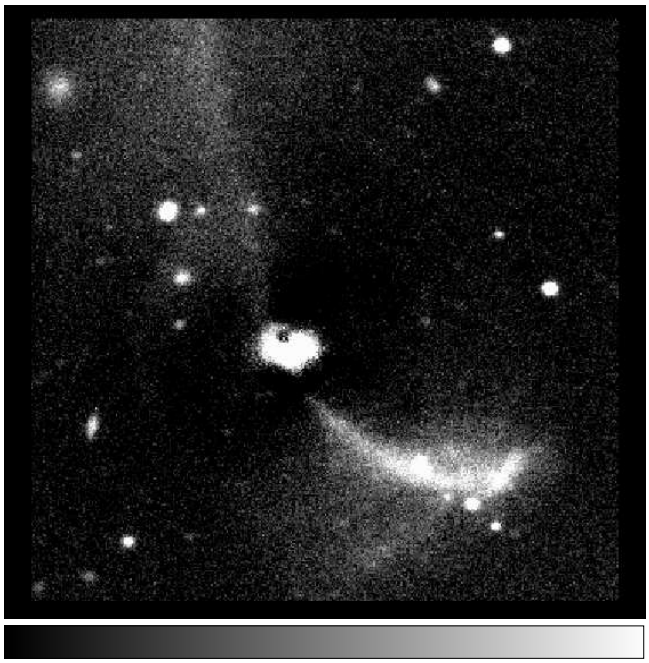

Fig. 5. B-band image of NGC5216 with the BUDDA best-fit bulge model subtracted. The area shown is 161×161 arcsec, with a linear intensity scale.

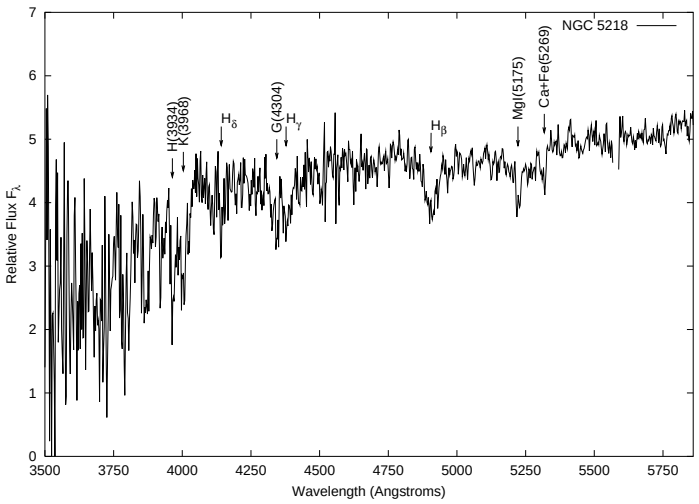

Fig. 6. Observed spectrum of NGC5218, from 7200s of Bolitas data (6 exposures), with detected lines labelled.

integrating each spectrum over the B-band response function and equating the mean value to the total B magnitude (Section 3). This gives one flux unit on Figure 6 corresponding to a flux from the whole galaxy of 0.95×10^{-14} ergs cm^{-2}s^{-1}Å^{-1} or luminosity 2.05×10^{39} ergs s^{-1}Å^{-1}, and on Figure 7, one unit is 1.20×10^{-14} ergs cm^{-2}s^{-1}Å^{-1} or luminosity 2.59×10^{39} ergs s^{-1}Å^{-1}.

Table 2 gives line equivalent widths, estimated using IRAF 'splot', for both spectra. The statistical significance of each line is estimated by summing in quadrature our inter-exposure error function over the FWHM of the line and dividing this by the integrated line profile. For both galaxies, we do not detect any emission lines for either galaxy, but do find strong absorption lines. The most obvious difference between the two spectra is that NGC5218 has much stronger Balmer absorption lines: $H\delta$, $H\gamma$ and $H\beta$, of which the last two are significantly broadened, with approximate FWHM of 28 and 45 Å, compared to the instrumental resolution of FWHM $\simeq$ 16–18$\mathring{A}$. NGC5216 has much weaker Balmer lines, with only $H\beta$ detected, but its other absorption lines are stronger than in NGC5218, as expected for an earlier Hubble type.

In NGC5216, the absence of emission lines indicating star-formation is not surprising in view of the lack of HI in the galaxy (Hibbard 2001).

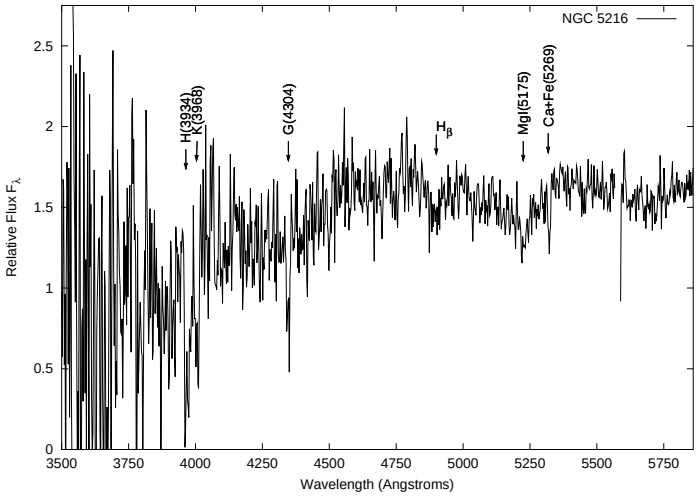

Fig. 7. Observed spectrum of NGC5216, from 4800s of Bolitas data (4 exposures), with detected lines labelled.

TABLE 1

TABLE 2

Line	Equivalent width Å	
	NGC5218	NGC5216
[OII]3727	$< 5^*$	$< 10^*$
K(3934)	5.40 ± 0.70	15.3 ± 2.3
H(3968)	6.00 ± 0.73	9.84 ± 1.88
Hδ(4102)	2.92 ± 0.60	$< 2.4^*$
G(4304)	4.13 ± 0.90	6.48 ± 0.87
Hγ(4340)	4.47 ± 1.04	$< 2.4^*$
Hβ(4861)	8.01 ± 1.04	3.74 ± 1.46
[OIII]5007	$< 1.5^*$	$< 1.6^*$
Mg(5175)	3.33 ± 0.52	5.33 ± 1.06
Ca+Fe(5269)	2.08 ± 0.85	1.87 ± 0.73

* 2σ upper limits

However, NGC5218 is gas rich and an IRAS detection with the FIR flux apparently corresponding to a SFR of 3.9 $M_\odot yr^{-1}$. On the basis of our approximate 'absolute calibration', our estimated upper limit EW([OII]3727) $<$ 5Å for NGC5218 means F([OII]3727) $< 1.3 \times 10^{-13}$ ergs $cm^{-2}s^{-1}$ and a luminosity $L_{[OII]} < 2.8 \times 10^{40}$ ergs s^{-1}, and EW([OIII]5007) $<$ 1.5Å means F([OIII]5007) $< 6.4 \times 10^{-14}$ ergs $cm^{-2}s^{-1}$ and a luminosity $L_{[OIII]} < 1.4 \times 10^{40}$ ergs s^{-1}. From Kennicutt (1998), SFR $\simeq 1.4 \times 10^{-41} L_{[OII]}$, so in the absence of dust extinction, the SFR is $< 0.4 M_\odot yr^{-1}$. The [OIII] flux depends on factors such as metallicity, as well as SFR, but typically F([OIII]5007) $\simeq$ 1–2F(H_β) $\simeq$ 0.3–0.7F(H_α), and from Kennicutt (1998), SFR $\simeq 7.9 \times 10^{-42} L_{H_\alpha}$ giving the upper limit 0.16–0.37 $M_\odot yr^{-1}$. Hence our non-detection of emission lines from NGC5218, would require that the FIR emission is from a source other than young stars, i.e. an obscured AGN, and/or that star-formation in NGC5218 is subject to heavy dust extinction, $A_V > 2.5$ mag.

We compare the spectra of NGC5218 and NGC5216 with observed local galaxy spectra from the database of Storchi-Bergman, Calzetti and Kinney (2004), and with model spectra (Jimenez et al. 2004) representing evolving stellar populations at ages from 1 Myr to 13 Gyr. Comparing NGC5218 with M31 (NGC224), which is also Sb type (but not barred or interacting), we find that NGC5218 has Balmer lines about 3 times as strong (and broader), and it is also somewhat bluer (more UV continuum). Strong/broad Balmer lines indicate the galaxy has an enhanced content of type 'A' stars, and imply that it underwent a major burst of star-formation between 0.09 and 1.0 Gyr ago (e.g. Gonzáles Delgado, Lietherer and Heckman 1999).

We fit the observed spectrum of NGC5218 with a two-component model, consisting of a sum of the observed M31 spectrum (representing the pre-interaction galaxy) and a Jimenez et al. (2004) model for a single age stellar population of solar metallicity (representing the recent starburst), both redshifted to $z = 0.0098$. This model is parameterized in terms of T_{sb}, the age of the starburst, and f_{sb}, the starburst component's fraction of the total flux at $\lambda_{restframe} = 4500$Å. We fit by minimizing χ^2, weighting each point using the inter-exposure errors.

The best-fit (reduced $\chi^2 = 1.22$) is found for $T_{sb} = 0.1^{+0.1}_{-0.04}$ Gyr and $f_{sb} = 0.57 \pm 0.03$. However, this age could be an underestimate if M31 is slightly too red a template. The broadness of the $H\beta$ line favours a greater age, and a model fit to the $H\beta$ profile in isolation gives an age 0.4 ± 0.2 Gyr. We therefore adopt the intermediate age 0.2 Gyr as our best estimate, with $f_{sb} = 0.54$ (the best-fit for this age). Figure 8 shows this model, illustrating how the sum of these two components closely approaches the observed spectrum.

The starburst, in order to produce 54% of the present-day blue flux, would have absolute magnitude $M_B \simeq -19.53$, which for the Jimenez et al (2004) model of age 0.2 Gyr and Salpeter IMF would require a stellar mass 3.2×10^9 $M_\odot$. By comparison, the total luminosity of NGC5218 is $1.8 \times 10^{10} L_\odot$, and from the model of Bell and de Jong (2001), for a spiral with $B - R = 1.25$ the stellar $M/L_B \simeq 2.2$, giving $\sim 4 \times 10^{10} M_\odot$. From this we estimate that of order 8% of the current stellar mass was formed in the burst.

If the burst duration was $\sim$ 100 Myr, its mean SFR would have been $\sim$ 32 $M_\odot yr^{-1}$), about an order of magnitude greater than either the FIR upper limit for the current SFR (3.9 $M_\odot yr^{-1}$), or the time-averaged SFR (stellar mass/galaxy age) for the whole galaxy ($\simeq$ 3–4 $M_\odot yr^{-1}$). Hence HGC5218 underwent a major starburst, but neveretheless this consumed only a fraction of the total gas content of the pre-interaction galaxy, as NGC5218 is still very gas rich with $M_{HI+H_2} \simeq 1.47 \times 10^{10} M_\odot$ (Cullen, Alexander and Clemens 2003, 2006).

We fit the observed spectrum of NGC5216 with a combination of the observed spectrum of M32, a non-interacting elliptical without recent star-formation, and the Jimenez et al (2004) single age population. The best-fit model (reduced $\chi^2 = 1.15$) has $T_{sb} = 0.040^{+0.060}_{-0.025}$ Gyr and $f_{sb} = 0.37 \pm 0.06$. Ages > 0.1 Gyr are excluded, and would cause stronger Balmer lines than observed. Figure 9 shows the best-

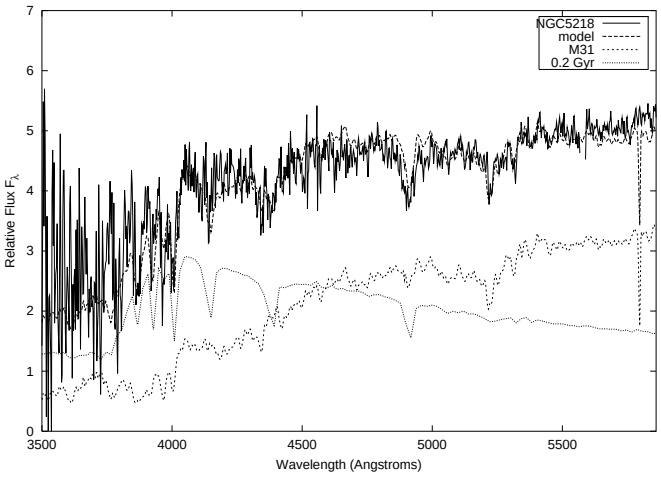

Fig. 8. Observed spectrum of NGC5218 (solid) together with a best-fitting model (heavy-dashed) which is a normalized sum of the observed spectrum of M31 (Storchi-Bergman et al. 2004: light-dashed) and a model spectrum for a 0.2 Gyr age stellar population (Jimenez et al. 2004; dotted).

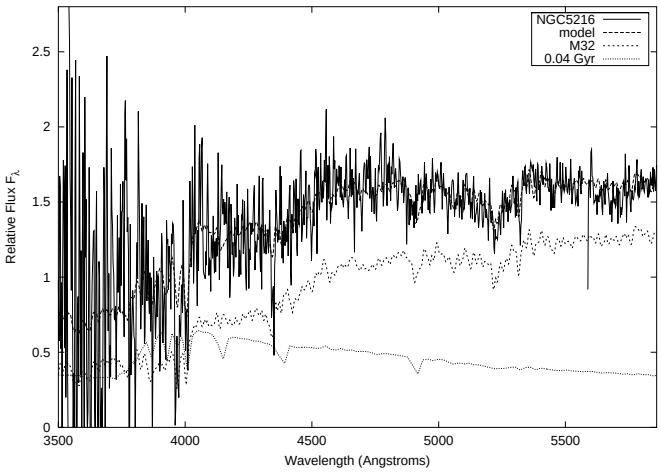

Fig. 9. Observed spectrum of NGC5216 (solid) together with a best-fitting model (heavy-dashed) which is a normalized sum of the observed spectrum of M32 (Storchi-Bergman et al. 2004: light-dashed) and a model spectrum for a 0.04 Gyr age stellar population (Jimenez et al. 2004; dotted).

fit model. Here the starburst component would have $M_B = -18.22$ and a stellar mass $2.56 \times 10^8 M_\odot$.

5. COLOURS

Using 'isophot.ellipse' we can measure, on the R and U images, the mean SB on the set of isophotes previously fitted on the B-band image. The difference in two passbands' SBs for each isophote will then give its colour $U-B$ or $B-R$. Figure 10 plots isophote colour against r_{sm} for the two galaxies. For NGC5216, we also measure the isophote SBs and colours with the bridge/plume (including the section passing through the galaxy) masked out in all passbands. This is to determine the colour of the body of the spheroidal, without 'contamination' from the interpenetrating bridge/plume, which might be very different in colour.

Both galaxies are significantly bluer at larger radii, in both colors. The spiral NGC5218 has a much stronger $B-R$ gradient than NGC5216; compared to the spheroidal it is about 0.26 mag redder at its centre but is bluer at all $r_{sm} > 17$ arcsec. However,in $U-B$, the spheroidal NGC5216 shows the stronger colour gradient, and outside of its central $r_{sm} \sim 3$ arcsec is bluer than NGC5218. We also see that masking out the bridge/plume passing through NGC5216 has little effect on its isophotal colours, producing only a very slight reddening. This confirms that the strong $U-B$ gradient and blueness of NGC5216 are intrinsic to its own stellar content and not due to blue flux from the plume.

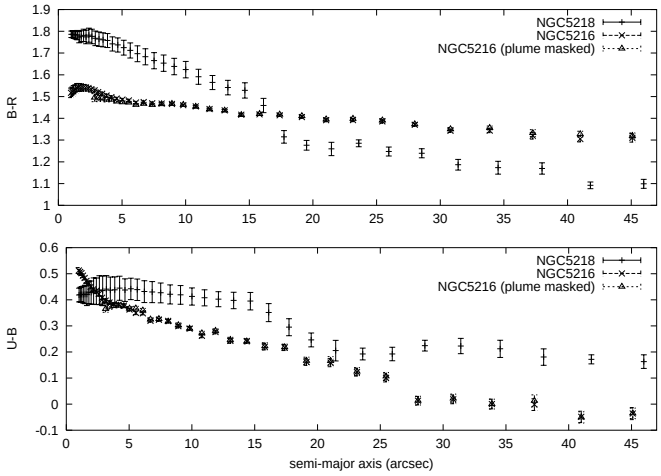

Fig. 10. Colours (a)$B-R$ and (b) $U-B$ of isophotes as a function of semi-major axis, for NGC5218, NGC5216, and NGC5216 with the bridge/plume masked out

.

Using polygon photometry (IRAF 'polyphot') we measure $B = 16.46$, $B - R = 0.65$ and $U - B = 0.12$ for the central part of the bridge, which is much bluer than the integrated colours of either galaxy. For the bright plume curving SW from NGC5216 (excluding the part < 33 arcsec from the galaxy centre, to reduce its contamination of the colours) we measure $B = 17.53$ with $B - R = 1.04$ and $U - B = -0.16$, again much bluer than either of the galaxies. For the tip of the plume only (from the 'bend' to its final end) we measure $B = 18.72$ with similar colours $B - R = 0.86$, $U - B = -0.14$. We note the plume is redder in $B - R$ but bluer in $U - B$ than the bridge.

We calculate $U - B$ and $B - R$ colours for the Jimenez et al. (2004) single-age, solar metallicity model spectra redshifted to $z = 0.0098$, for all ages 0.001 to 14 Gyr. Figure 11 shows the locus of model colours together with the observed colours (integrated and for individual isophotes) of the two galaxies and of the tidal features.

The integrated colours of NGC5216 are similar to a single 5 Gyr age stellar population, but also lie on a straight line between ~ 10 Gyr age and very young (0.02–0.04) Gyr stars, and hence could be produced by a mixture of these, as our fit to the spectrum suggests. The integrated colour of NGC5218 cannot be fitted by any single age model, but is consistent with a mixture of old (≥ 5 Gyr) and 0.2–0.4 Gyr age stars, again in agreement with our interpretation of its spectrum. The bridge colours closely match a pure 0.4 Gyr old population. However, the plume colours are more consistent with a mixture of very old stars (which were probably carried out of NGC5216) and a greater number of extremely young (~ 0.02 Gyr) stars. Considering that the plume, unlike NGC5216, corresponds to a concentration of HI, it could still be a site of star-forming activity.

Looking at the colours of the individual isophotes, the red centre of NGC5218 has the colour of 5–14 Gyr old stars with dust reddening of about 0.2 in $B - R$. With increasing radius the isophote colour gradually shifts bluewards towards that of the bridge, or a 0.2–0.4 Gyr age population. The central colours of NGC5216 are consitent with very old (> 10 Gyr) stars, but with no requirement for dust-reddening. With increasing radius the isophotal colour shifts rapidly bluewards in a direction indicating an increasing relative contribution of very young (0.02–0.04 Gyr) stars. We can see from Figure 11 how the younger age of the young stars in NGC5216, compared to NGC5218, can account for the spheroidal's stronger $U - B$ colour gradient, despite its weaker $B - R$ gradient. From age 0.02 Gyr to 0.4 Gyr the models show much reddening in $U-B$, from -0.47 to +0.10, but little change in $B-R$, from 0.58 to 0.68. We note again that the young stars are present in the body of NGC5216 and not just the bridge/plume.

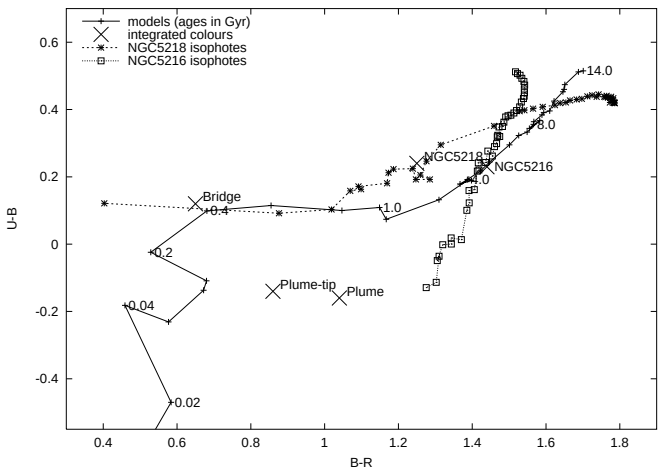

Fig. 11. $B - R$ against $U - B$ colours for Jimenez et al. (2004) single-age models, ages labelled in Gyr; integrated colours of the two galaxies and some tidal features; and the loci of the isophotal colours for the two galaxies, in both cases running from the galaxy centres at the top left (reddest), to the outermost edges at the bottom right (bluest)

In summary, the tidal features in the Arp 104 system are blue, as we would expect, but the most unusual features of the colours are (i) the redness of the NGC5218 nucleus, implying dust, and (ii) the blueness (outside the nucleus) of the spheroidal NGC5216, implying very recent star-formation.

6. DISCUSSION AND CONCLUSIONS

We have obtained UBR imaging and optical spectroscopy of the interacting galaxy pair Arp 104 (NGC5218 and NGC5216). Examining the profiles we confirm that NGC5218 is a disk galaxy with a substantial bulge component ($B/D \simeq 0.43$) and that NGC5216 is a de Vaucouleurs profile E0 For both galaxies, we detect no emission lines, and, in the absence of dust extinction estimate upper limits to the SFRs of 0.2–0.4 $M_{\odot}yr^{-1}$. Cullen, Alexander and Clemens (2003) do claim a detection of Hα emission for NGC5218, but with a very low luminosity implying a SFR ~ 0.05 $M_{\odot}yr^{-1}$.

However, the FIR luminosity of NGC5218 may be evidence of a SFR of up to 3.9 $M_{\odot}yr^{-1}$, and the galaxy contains a large mass of hydrogen, $M_{\rm HI+H_2} \simeq 1.47{\times}10^{10} M_{\odot}$ (Cullen, Alexander and Clemens 2003, 2006). Furthermore the very red colours of the in-

ner ~ 10 arcsec, up to $\Delta(B-R) \simeq 0.2$ mag redder than 10 Gyr old stellar population, imply there is some dust reddening. The red region corresponds to the molecular gas bar described by Olsson, Aalto and Hüttemeister (2005). Hence it seems possible there is ongoing star-formation of anything up to 3.9 $M_{\odot}yr^{-1}$ occurring deep in this nucleus or bar, with heavy extinction of $A_V > 2.5$ mag. Alternatively some or most of the FIR emission may be from a dust-shrouded AGN. Mid infra-red spectroscopy might distinguish the two.

Whether or not NGC5218 is currently forming stars, it seems to have undergone a burst of much more intense star-formation (an order of magnitude above the time-averaged SFR) at an earlier stage in its interaction, probably at or shortly after the perigalacticon with NGC5216, an estimated 0.3 Gyr ago (Cullen, Alexander and Clemens 2006). Firstly, the spectrum shows strong Balmer absorption lines, especially $H\beta$, consistent with a major starburst 0.2–0.4 Gyr ago; from our model fit to the spectrum we estimated the mass of stars formed as $3.2 \times 10^9 M_{\odot}$. Secondly, both the inclined outer shell around the disk of NGC5218, and the bridge connecting the two galaxies, have colours consistent with the same age, 0.2–0.4 Gyr. The close passage must have disrupted the disk, triggered starbursting within it and created the shell, and then as the two galaxies separated in their orbit, NGC5216 pulled away substantial amounts of gas from NGC5218 together with newly formed blue stars from the shell or outer disk, forming the bridge.

Comparing the spectrum of NGC5216 with the elliptical M32, it shows an excess of blue/UV flux, suggesting the presence of young stars, but the Balmer lines are not especially strong, favouring a younger age < 0.1 Gyr. We best-fit our spectrum with a ~ 40 Myr age starburst of much lower mass ($2.56 \times 10^8 M_{\odot}$) than in the spiral. In moving the ~ 50 kpc from one galaxy to the other in ~ 0.2 Gyr, the focus of star-formation has moved at ~ 240 km s^{-1}, about the rotation velocity of the spiral. The $U-B$ profile of NGC5216 suggests these young stars are distributed throughout the body of the spheroid but are more prominent at larger radii and much less so in the central ~ 3 arcsec, which is red.

The unusual presence of young stars in this E0-type - formed 0.2–0.3 Gyr after the close passage - can be explained if $\sim 2 \times 10^8 M_{\odot}$ of HI was transferred from the spiral, along the bridge to NGC5216, *refuelling* the spheroidal and resulting in a short-duration starburst. It is plausible that the burst in NGC5216 could have been fuelled entirely through the bridge, as similar bridges e.g. in NGC2992/3 (Duc et al. 2000) may contain the required HI mass in only $\sim 10kpc$ of length and evidence of spiral-to-elliptical cross-fuelling along tidal bridges, at rates ~ 2 $M_{\odot}yr^{-1}$, has been reported for other interacting pairs, such as Arp 105 (Duc et al. 1997). NGC5216 now shows no emission lines and contains very little HI or H_2, and our spectra and photometry support the suggestion of Cullen, Alexander and Clemens (2006) that cross-fuelling did occur in this system but that the transferred gas has all been exhausted.

However, some gas, rather than forming stars within NGC5216, appears to have passed through and out of the galaxy, where the bridge becomes the SW. The plume is very blue in $U-B$ implying its stellar content is dominated by a very young (< 40 Myr) stellar population, perhaps with a smaller content of old stars. The tip of the plume, 60–70 arcsec from the nucleus of NGC5216, is broadened and the HI map shows a concentration of HI, resembling the HI peak at the end of the NGC2992 tidal tail (Duc et al. 2000), which is both a star-forming region and a formative tidal dwarf galaxy. Extrapolating the estimated rate of movement of the focus of star-formation, from the centre of NGC5216 it would take ~ 50 Myr to reach the plume tip, which takes us to approximately the present day and so is consistent with the plume tip being the current site of star-formation in the system. The apparent magnitude we measure for the plume tip corresponds to $M_B \simeq -14.43$, which for an age ~ 0.04 Gyr is a stellar mass of only $\sim 10^7 M_{\odot}$. Hence if this is a tidal dwarf galaxy, which typically have virial masses $\sim 10^9 M_{\odot}$ (e.g. Braine et al. 2001), it is mostly gas, and in a very early stage of its star-formation.

To verify the existence of a formative tidal dwarf galaxy at the plume tip, observing in Hα with a Fabry-Perot or another instrument of high velocity resolution (e.g. the Manchester Echelle Spectrography), could reveal the spatial extent of the current star-formation and whether the star-forming region shows the steep (~ 50 km s^{-1}) velocity gradient expected if the plume tip is sufficiently massive ($\sim 10^9$ $M_{\odot}$) and self-gravitating that it is destined to become an independent dwarf galaxy (e.g. Bournard et al. 2004). In several 10^8 yr NGC5216 and NGC5218 will experience another close encounter, perhaps this time colliding and merge, and could then eject the 'plume tip object' to become a separate galaxy.

NR acknowledges the support of the Universidad Nacional Autonoma de Mexico, and the help of all at the Observatorio Astronomico Nacional, San Pedro Martir, especially Michael Richer, in the observations described here.

REFERENCES

Arp H., 'Atlas of Peculiar Galaxies', 1966, ApJS, 14, 1.
Barnes J.E., 2004, MNRAS 350, 798.
Bell E.F., de Jong R.S., 2001, ApJ, 550, 212.
Bournaud F., Duc P.-A., Amram P., Combes F., Gach, J.-L., 2004, A&A, 425, 813.
Braine J., Duc P.-A., Lisenfeld U., Charmandaris V., Vallejo O., Leon, S., Brinks E., 2001, A&A, 378, 51.
Cullen H., Alexander P., Clemens M., 2003, Astrophysics and Space Science, 284, 503.
Cullen H., Alexander P., Clemens M., 2006, MNRAS, 366, 49.
Duc P.-A., Brinks E., Wink J. E., Mirabel I. F., 1997, A&A, 326, 537.
Duc, P.-A., Brinks, E., Springel, V., et al. 2000, AJ, 120, 1238
Gonzáles Delgado R.M, Leitherer C., Heckman T.M., 1999, ApJSS, 125, 489.
Hamuy M., Suntzeff N.B., Heathcote S.R., Walker A.R., Gigoux P., Phillips M.M., 1994, PASP, 106, 566.
Giuricin G., Tektunali F.L., Monaco P., Mardirossian F, Mezzetti M., 1995, ApJ, 450, 41.
de Grijs R., Lee J.T., Clemencia Mora Herrera M., Fritze-v. Alvansleben U., Anders P., 2003, New Astronomy, 8, 155.
Helou G., Soifer B.T., Rowan-Robinson M., 1985, ApJ, 298, L7.
Hibbard J.E., van Gorkom J.H., Rupen M.P., Schiminovich D., 2001, ASP Conf Series 240, 'Gas and Galaxy Evolution', 657.
Keenan P.C., 1935, ApJ, 81, 355.
Kennicutt R.C, 1998, ApJ, 498, 541.
Landolt A.U., 1992, AJ, 104, 340.
Olsson E., Aalto S., Thomasson M., Hüttemeister S, 2004, Astronomical Society of the Pacific vol 320 'The Neutral ISM in Starburst Galaxies', 162.
de Souza R.E, Gadotti D.A., dos Anjos S., 2004, ApJSS, 153, 411.
Kurtz, S., Churchwell, E., & Wood, D. O. S. 1994, ApJS, 91, 659
MacLeod, G. C., van der Walt, D. J., North, A., Gaylard, M. J., Galt, J. A., & Moriarty-Schieven, G. H. 1998, AJ, 116, 2936
Odegard, N. 1986, AJ, 92, 1372
Öpik, E. J. 1953, Irish Astron. J., 2, 219
Palla, F., Brand, J., Cesaroni, R., Comoretto, G, & Felli, M. 1991, A&A, 246, 249
Rengarajan, T. N., Verma, R. P., & Iyengar, K. V. K. 1989, MNRAS, 237, 1047
Reynoso, E. M., & Mangum, J. G., 2001, AJ, 121, 347
Taylor, J. H., Manchester, R. N., & Lyne, A. G. 1993, ApJS, 88, 529
Velázquez, P. F., Kurtz, S. E., Dubner, G. M., Goss, W. M., & Holdaway, M. A. 2002, submitted to AJ

Full addresses go here